Marine Structures 88 (2023) 103368

Contents lists available at ScienceDirect

Marine Structures

journal homepage: www.elsevier.com/locate/marstruc

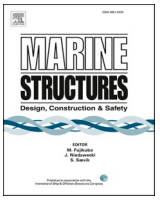

Validation of earthquake analysis methodology of a suction-caisson foundation-structure through model testing

Siamak Feizi [a,*], Knut Arnesen [b], Andreas Aaslid [b], Jens Bergan-Haavik [b], Jan Helge Hassel [c], Stephen Kulleseid [c], Armin Ghadak [d]

[a] Norwegian Geotechnical Institute, NGI (Former DNV), Sognsvn 72, 0855, Oslo, Norway
[b] DNV, Veritasveien 1, 1363, Hovik, Norway
[c] TechnipFMC, Kirkegårdsveien 45, 3616, Kongsberg, Norway
[d] British Petroleum (BP), London, UK

ARTICLE INFO

Keywords:
Shah deniz
Earthquake analysis
Suction-caisson foundation
Model test
Soil model calibration

ABSTRACT

Suction caissons are one of the most widely used foundation solutions for subsea structures and wind farms. Seismic response of subsea structures is however seldom documented properly, often just treated as a foundation capacity issue applying a quasi-static acceleration and not considering the inertial interaction between the structure and the soil. The more relevant tasks to document are the motions of the unit and the response of the externally connected flowlines and equipment/systems on the unit.

Based on a case study located in the Shah Deniz field in the Caspian Sea, model centrifuge tests and numerical modelling were carried out to validate the global response of a 4-caisson supported manifold structure subject to seismic motions in soft clay. The centrifuge tests were carried out at 58 g at the centre for geotechnical modelling at UC Davis. To simulate the soil-structure interaction, a series of non-linear springs defined by kinematic hardening models were used in analyses with the ABAQUS software. This development includes the algorithms for determining the required model parameters. A very good agreement between recorded response from the centrifuge test and calculated response from the FE-analyses was achieved.

The development and validation of the soil model presented in this paper is an improvement in design methodology for caisson foundations subjected to earthquake loading. The non-linear soil springs are well suited to incorporate in more detailed structural analyses where an accurate representation of the foundation response is required. The paper also briefly describes how the subsequent earthquake design analyses were performed for the Shah Deniz manifold structures making use of the validated soil spring model and the added value it gave to the project.

1. Introduction

In recent years, suction caissons have widely been used as one of the main foundation alternatives in the offshore industry such as foundations for subsea structures and wind turbines. These foundations are installed by combination of the self-weight of the structure and a suction pressure applied inside the caisson. Most publications, for example studies done by Refs. [1–6]; [7] and [8] has mainly

* Corresponding author.
E-mail address: Siamak.feizi@ngi.no (S. Feizi).

https://doi.org/10.1016/j.marstruc.2023.103368
Received 8 September 2021; Received in revised form 3 September 2022; Accepted 18 December 2022
Available online 17 January 2023

focused on the numerical simulation and the foundation response to loads or combination of loads treated as external loads acting upon the structure. Model testing such as centrifuge tests have been used by many researchers to study the installation process [9–11] and [12], cyclic performance [5], tension capacity [13]; and [14] and nonlinear lateral stiffness and bearing capacity of suction caissons [15]. Many of these have been successfully back analysed using numerical modelling methods. However, there are limited publications (e.g Ref. [16] related to the seismic performance of caisson-supported structures.

Earthquake design of subsea structures are often treated as a foundation capacity issue, e.g. multiplying dynamic masses with maximum spectral acceleration from an earthquake design spectrum representing the seabed motions. However, when such checks conclude with foundation failure, it is just an indication that the soil may be highly utilised and that the associated displacements need to be determined. The earthquake response of a structure embedded in soil will depend on the dynamic soil-structure interaction governed by the mass, stiffness and damping characteristics of the system. Non-linear soil behaviour may therefore change the structural response, inertial loads and corresponding displacements. When the soil is susceptible to cyclic degradation, seismic action could lead to a foundation failure due to externally acting loads. For foundations like monopiles supporting structures with significant masses at high elevation (e.g. wind turbines) large rotations can develop during an earthquake, driven also by second order moments from mass eccentricities as the foundation rotates, or for a wind turbine loaded simultaneously from operational wind forces on the blades. For subsea structures, the focus related to earthquake response is in displacements and accelerations which may influence connected flowlines and equipment. It may also be important to check that any dynamically sensitive systems, e.g. piping systems and valves, do not have eigen periods that coincides with the main oscillation period of the subsea structure.

These earthquake design issues for subsea structures were identified for the manifolds at the Shah Deniz gas field. The field was discovered in 1999. It is located on the deep-water shelf of the Caspian Sea, 70 km south-east of Baku, in water depths ranging from 50 to 500 m. Shah Deniz development is a mega project and is one of the largest gas developments in the world. The Shah Deniz development consists of several locations at varying water depths with single production wells tied back to manifold structures. From the manifolds the gas is further transmitted through flowlines to a production jacket platform at more shallow waters and from there through pipeline to shore. The site is seismically active. It was therefore of importance to understand the earthquake response of the manifolds and its interactions with other components of the development.

The foundation of the manifold consisted of four suction caissons connected to a main support frame. As previously stated, there have been limited studies and publications on the seismic performance of caisson-supported structures. To gain confidence of the seismic analyses and design, the field developer, BP, initiated centrifuge tests to be performed with the aim to.

- determine the global seismic response of the 4-caisson-supported manifold structure in a soft clay, similar to the clay located at Shah Deniz field.
- validate a soil model for time series analysis based on the performance of the manifold in the centrifuge tests

The purpose of the centrifuge test was hence to validate the non-linear soil model (backbone curve and unloading-reloading behaviour including hysteretic damping) by capturing the global response of the soil-structure system to earthquake loading. In the project the non-linear soil model was subsequently included in a more detailed structural model where piping systems, valves and connected flowlines and well jumpers were also included. Structural details were left out of the centrifuge tests. The mass of piping and other dynamically sensitive equipment on the manifold is very low compared to the total dynamic mass. Accordingly, the dynamic motion of those has no significant influence on global motions. However, the soil conditions, overall structural dimensions and mass distribution were important to match as close as possible to the project data.

It is not possible to include all elements of importance and interest for the earthquake response of the manifold in a centrifuge test. E.g. the interaction with water through added mass and water damping cannot be accounted for by centrifuge tests, but needs to be accounted for in the design. In addition, the soil in the model test has somewhat different characteristics compared to the field location. Dynamic response of piping and other equipment is not possible to verify from centrifuge tests. This was done as part of the design work for the Shah Deniz manifold, where a detailed model of the manifold structure, the piping and other equipment was included.

The centrifuge tests were conducted at UC Davis Centre for Geotechnical Modelling (CGM) in California, using their 9 m radius centrifuge that includes a shaking table being able to simulate earthquake. The tests were performed at 58 g. This paper documents the FE-analysis and compares obtained response with measured responses from model tests. The paper also briefly describes how the subsequent earthquake design analyses were performed for the Shah Deniz manifold structures making use of the validated soil spring model and the added value it gave to the project.

2. The centrifuge test

The centrifuge model dimensions of the caisson foundation matched those of the Shah Deniz manifold structure and the structural mass distribution, i.e. total mass, CoG and mass moment of inertia matched well with the Shah Deniz manifold. Input free field motions to the FE-analysis of the centrifuge model were the accelerometer recordings available at several levels in the centrifuge soil. These motions were applied to the far boundary of the soil springs.

2.1. The manifold structure

The prototype model of the manifold structure was fabricated from aluminium alloy designed to replicate as good as possible dimensions and mass distributions of the manifold designed for Shah Deniz. Light and at the same time stiff profiles like aluminum

alloy are however often chosen to use in small-scale model tests as the model dimensions (following the scaling laws) then become more practical than would be the case for steel.

Structural characteristics of the prototype model are.

- Structural mass above foundations of 780t with CoG (Centre of Gravity) at the centre axis 4.5 m above mudline
- Foundation caisson dimensions: OD (diameter) = 5.89 m, L (length) = 16.1 m. Centre to centre distance = 9.7 m.
- Structural mass per caisson = 116t, mass of entrapped soil per caisson = 820t

Mass moments of inertia at the CoG for the structural parts above the foundation were accounted for. Complying with the centrifuge model laws all dimensions are scaled down with a factor of 58, corresponding to the 58 g acceleration in the test. Correspondingly, the mass of the centrifuge model is scaled down by a factor 58^3 compared to the prototype.

The centrifuge model was assembled within the large "hinged plate" container (HPC). The HPC internal dimensions are 1756 mm by 649 mm and 516 mm deep. A rubber liner (3 mm thick) was placed within the container to prevent leakage of pore fluid. The centrifuge model layout showing locations of the manifold structure and global coordinate system is illustrated in Fig. 1.

The width of the foundation footprint is 15 m and the embedment is 16 m. The distance from the caisson edge to the container wall is 26 m. This assures that the container wall has no significant impact on the manifold response. Inside the liner on the north and south ends of the container, a series of vertical studding rods were installed to provide the required complementary shear stresses to avoid/limit reflecting waves effects at these boundaries.

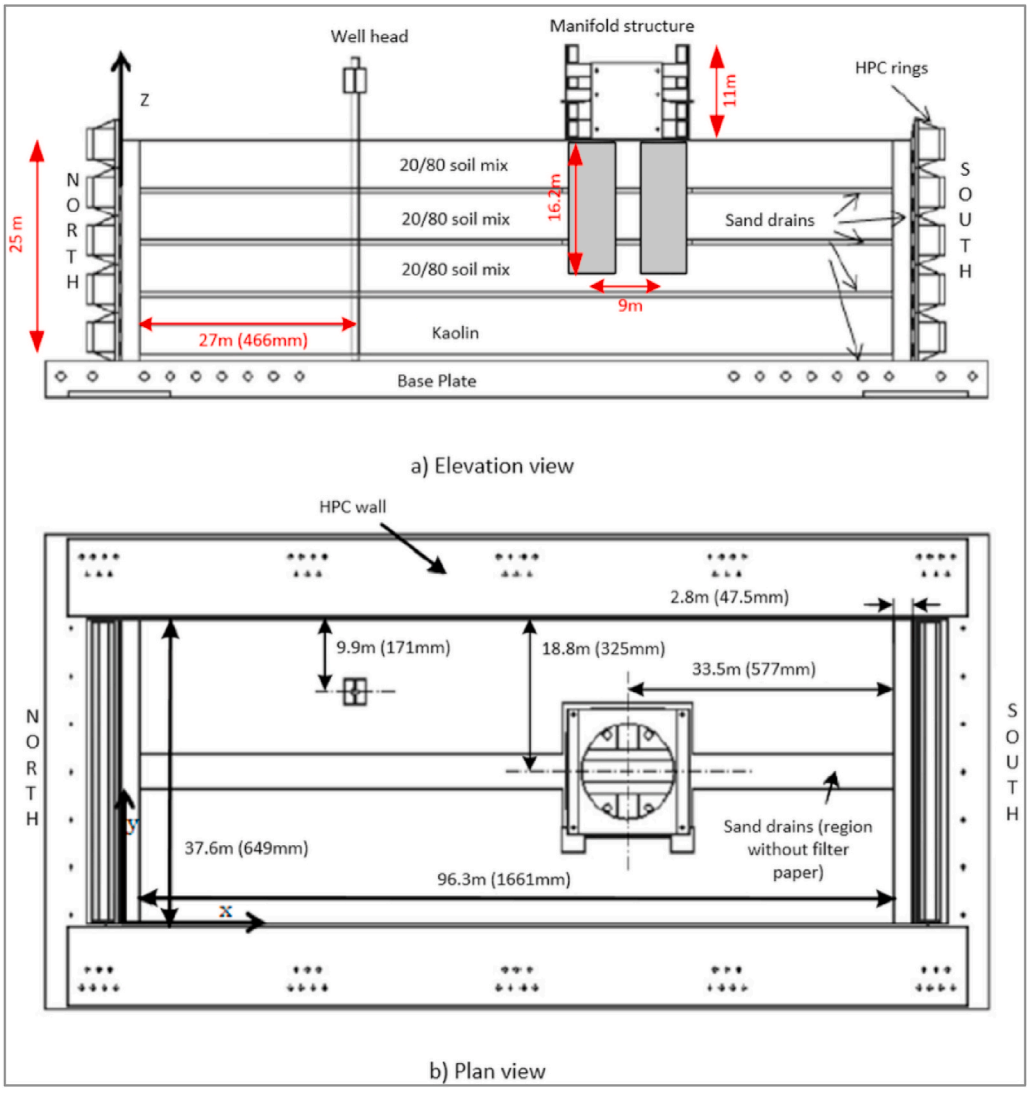

Fig. 1. Model layout.

2.2. Soil characteristics

The clay for the tests was constructed by consolidating a slurry mixture of kaolin and clay originating from the Shah Deniz field. The slurry consisted of 80% kaolin and 20% Shah Deniz clay. Mixing with Kaolin was performed in order to obtain a clay that could be consolidated within a reasonable time in the centrifuge tests. The clay was constructed in 8 lifts. In-between each second lift a thin sand layer was placed, being 5 mm thick. These layers were required to reduce the consolidation time. Consolidation was performed after filling each layer to establish a targeted shear strength profile. The soil was also consolidated at 58 g in order to establish the initial drained effective stresses prior to applying the earthquake excitation. The shear strength was tested by performing T-bar tests at 1 g condition prior to running the centrifuge and after consolidation at 58 g. Vane testing was also performed within the test chamber after 58 g consolidation. After the centrifuge tests, samples were taken for testing in the laboratory. Static and cyclic DSS tests were performed from the sampled soil, where the soil was consolidated to match the 'in situ' effective stresses. Based on these tests, the undrained shear strengths have been evaluated as presented in Fig. 2. For comparison, typical shear strengths at Shah Deniz field is shown on the same figure. As a result of mixing kaolin with the Shah Deniz clay for the centrifuge test, both submerged weight and plasticity is different. The centrifuge test clay had a submerged weight of 8 kN/m^3 compared to 3–5.5 kN/m^3 for the Shah Deniz clay increasing with depth. Plasticity for the centrifuge test clay was 18% compared to 65-40% for the Shah Deniz clay decreasing with depth. Due to the higher submerged weight of the centrifuge test clay, and the fact that the soil was consolidated for the overburden submerged weight, the shear strength became somewhat higher than for the Shah Deniz clay.

The properties of the tested clay are thus not fully comparable to the Shah Deniz clay. For the purpose of calibrating the soil model, this is not essential as long as relevant soil parameters required for the soil model were available, and both soils were normally consolidated clays. The results of the cyclic tests performed for the centrifuge clay was assessed and compared with the tests performed for the Shah Deniz clay and with the cyclic behaviour of the reference Drammen clay ([17]; [18]). The Drammen clay (which is referred in many publications) is a marine plastic clay with natural water content of 52%, clay content of 50%, specific gravity of 27 kN/m^3 and plasticity index of 27%, i.e. in between the clay for the centrifuge test and the clay at the Shah Deniz field.

The mixed soil used for the centrifuge tests is much more sensitive (higher ratio of intact to remoulded shear strength) than both the Drammen clay and the Shah Deniz clay, which is to be expected because of the much lower plasticity of the mixed clay. Based on the tests performed and correlations with Drammen Clay cyclic strength diagrams, a cyclic strength for 10 equivalent cycles was chosen as 0.7 times the static shear strength for the centrifuge test clay, compared to between 1.0 and 1.4 for Shah Deniz clay, as illustrated on Fig. 3. Thus, the difference in cyclic strength used as input to spring calculations is significantly lower than for the static strength.

2.3. Instrumentation of the centrifuge test

The response in the soil as well as in the structure were monitored throughout the tests. Soil motions were measured with accelerometers in the soil. In addition, pore pressures were monitored in each of the clay layers and in the sand bands between the clay layers. The manifold structure was instrumented with accelerometers and with linear potentiometers for measuring displacements.

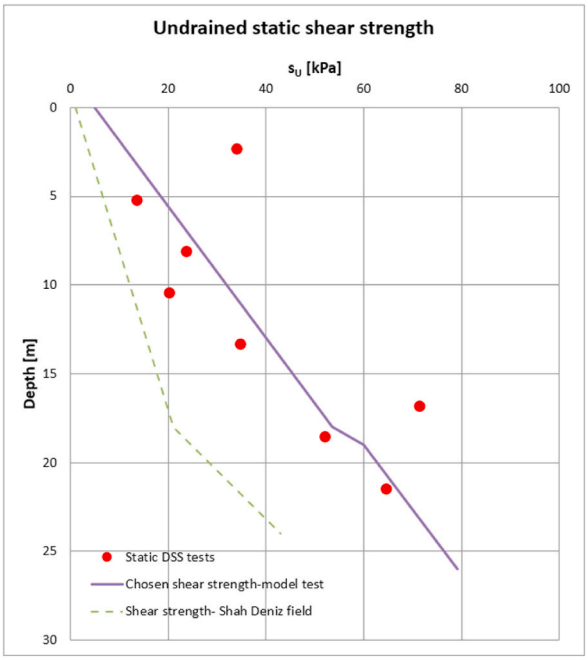

Fig. 2. Shear strength profile used in calculations.

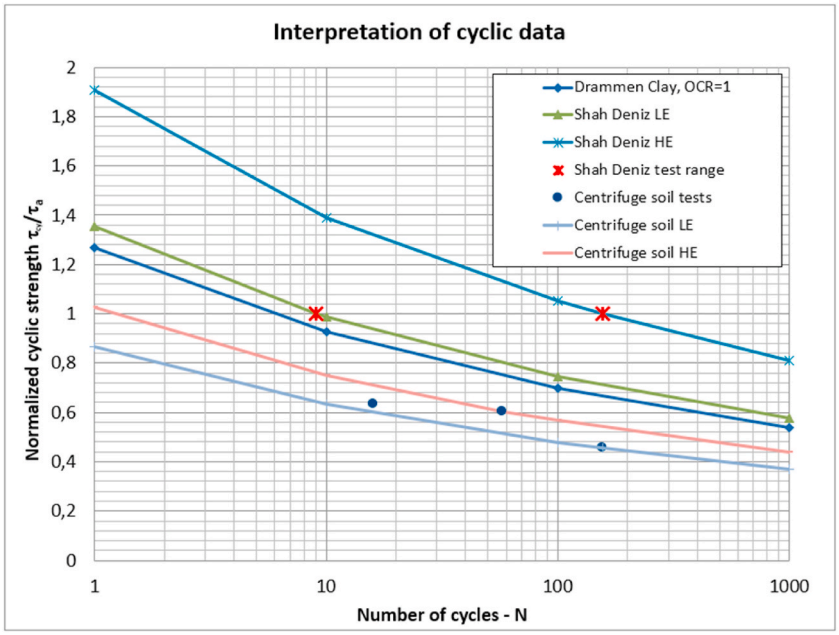

Fig. 3. Interpretation of cyclic strength.

The position of the instrumentation is shown in Fig. 4. The distance between the accelerometers #A1 to #A6 and the manifold structure was considered sufficient to regard the recorded motions as representative for the free field motions, i.e. unaffected by the interaction with the manifold structure. In the validation analyses, the records from these accelerometers are used as free field motions for the FEM analysis.

The manifold structure was installed at 1 g several days prior to spin-up. Penetration of the caissons was performed via the application of a large block mass, with the load being distributed through a series of wooden beams across the top bar of the manifold. A representative stage during the installation is shown in Fig. 5.

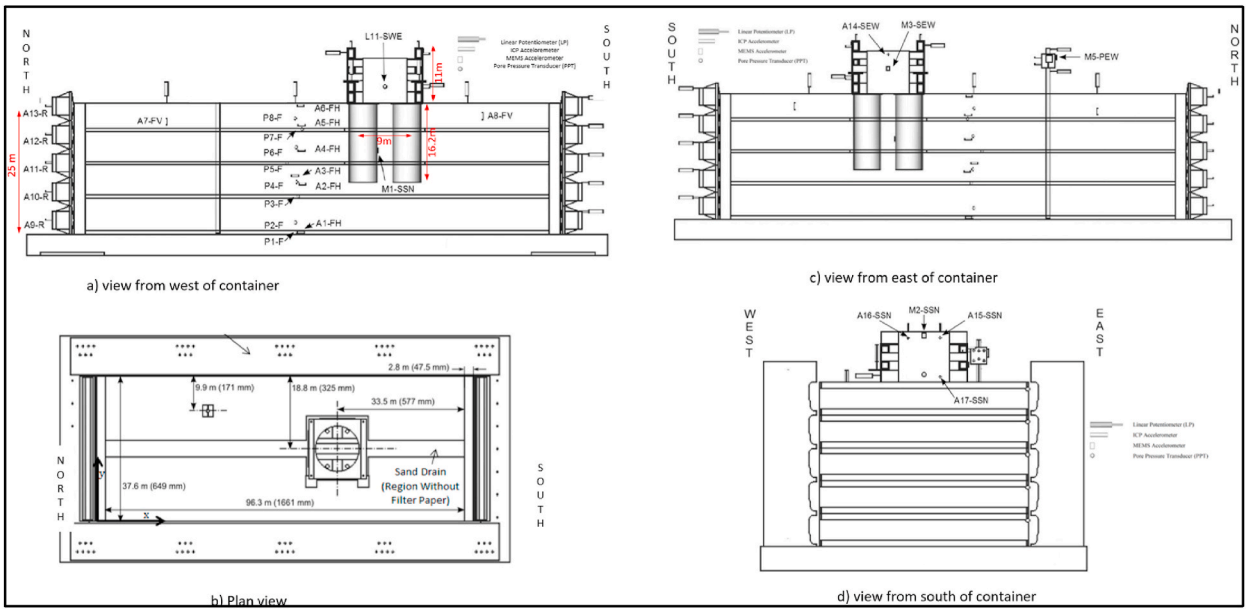

Fig. 4. Sensors layout.

2.4. Earthquake motions

The centrifuge tests were performed with input motions defined to represent two different levels of earthquake, the extreme level earthquake (ELE) and the abnormal level earthquake (ALE). The level of ELE and ALE motions were chosen to be comparable with the earthquake level at the Shah Deniz field. Whereas for the Shah Deniz design analysis seven different time histories scaled for the Shah Deniz field were analysed in accordance with the requirements of the ISO 19901–2 [19] code, only motions scaled from Northridge earthquake were applied in the centrifuge tests. The earthquake motions were applied in one horizontal direction, corresponding to the long axis of the test bin. The recorded motions in the soil are shown in Fig. 6 for the ALE case.

Fig. 7 shows a short time sequence of the recorded ALE motions. There is a notable phase difference in the free field motions at the various depths. This is due to the time for the motions to propagate vertically from the shaking table, similar to vertical propagation of motions from bedrock towards seabed at the real location. This phase difference is relevant to consider for earthquake analyses of structures supported on foundations deeply embedded in soft clays, where the shear wave velocity of the soil is low.

3. Numerical simulations

3.1. Earthquake motions input

In the ABAQUS model, the recorded input motions at free field are applied to the far boundary of the soil spring connecters according to the depths of the accelerometers and the depth of the spring connectors, as shown in Table 1.

3.2. Structural modelling

The earthquake response is determined performing time history analysis with ABAQUS [20]. The model consists of beam elements representing the caissons and spring elements representing the soil resistance. Modelling of the caisson by beam elements is industry practice when using p-y curve formulations. More advanced analyses could be performed by modelling the suction caisson by shell elements and the soil by continuum elements. This approach would however not be practical for the project as the analyses would be too time consuming when included together with other structural details required to suit the project requirements. Instead, detailed geotechnical finite element analyses using PLAXIS 3D [21] were performed to calibrate the simpler p-y curve approach, which finally was validated by the centrifuge test.

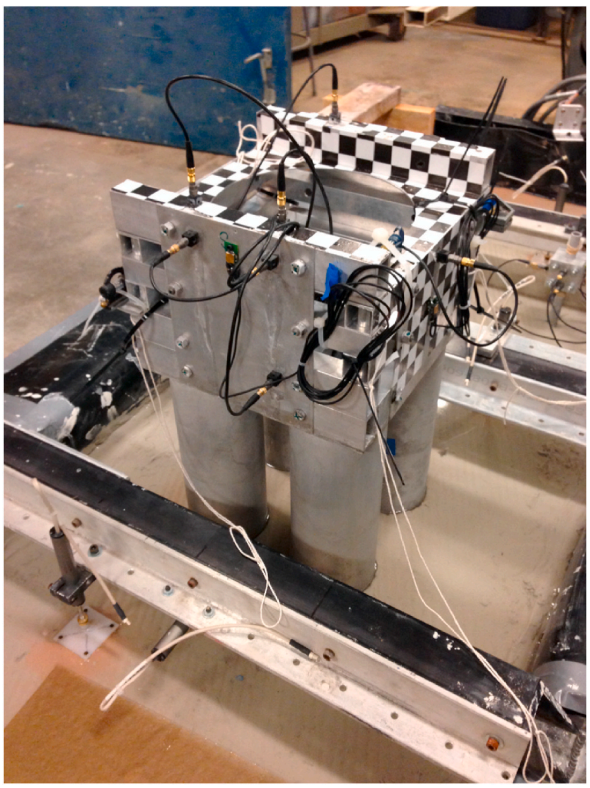

Fig. 5. Installation mechanism for the manifold structure.

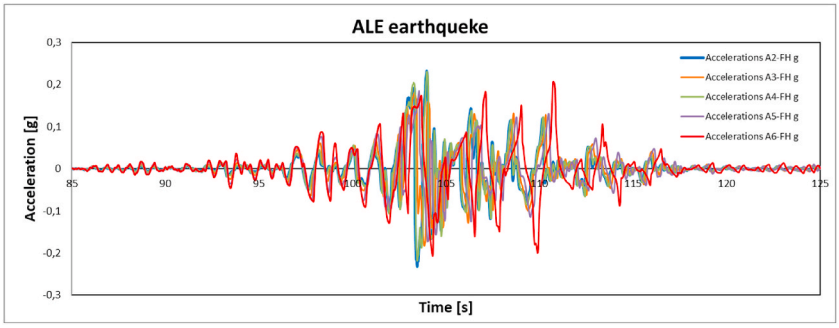

Fig. 6. Recorded free field motions- ALE.

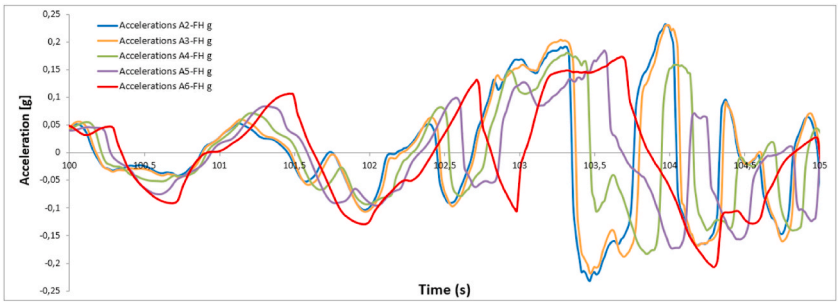

Fig. 7. Short sequence of recorded free field motions.

Table 1
Accelerometer locations used in FEM model.

Sensor	Sensor depth in centrifuge model [m]	In ABAQUS model
A6-FH	0.11	Applied at depths 1 and 2 m
A5-FH	3.72	Applied at depths 3, 4,5 and 6 m
A4-FH	8.92	Applied at depths 7, 8,9, 10 and 11 m
A3-FH	14.96	Applied at depths 12, 13,14and 15 m
A2-FH	16.05	Applied at the foundation tip level

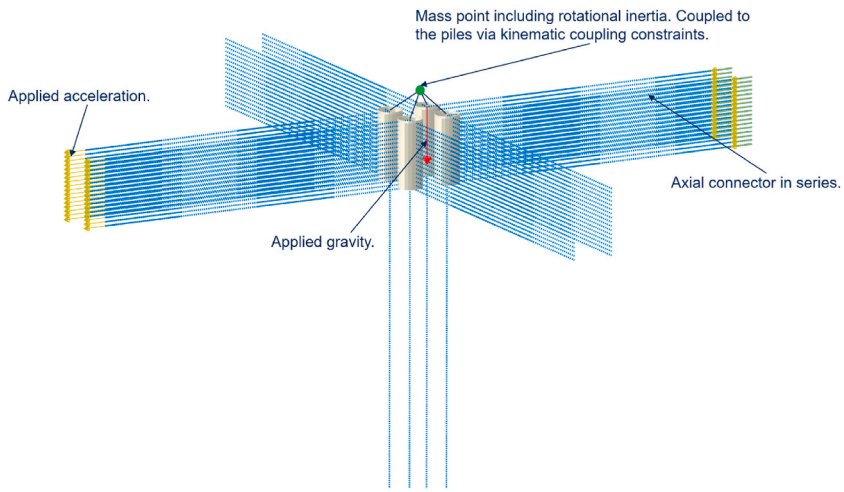

Fig. 8. Finite element model of the foundation caissons with soil springs.

To represent the mass of the manifold including its foundation base structure a concentrated point mass and corresponding mass moment of inertia (3 components) representative for the centrifuge structure was modelled at the centre of gravity of the manifold structure, as described in Chapter 2. The finite element model of the system is shown in Fig. 8. The foundation caissons were modelled as beams with a mass distribution along the axis of the beams that accounted for the structural mass of the caissons and the mass of entrapped soil inside the caissons. The latter is realistic and important to include. The soil inside the caissons is practically incompressible for undrained loading and will follow the motion of the caissons.

The points on the structure where motions were recorded in the centrifuge tests were in the analysis represented by coupling mass elements (insignificant mass used) to the COG. The test prototype was designed to behave as a rigid body; thus, the measurement points was included to ensure that the test prototype behaved as expected.

The input earthquake motions were applied to the far boundary of non-linear spring elements that represent the soil stiffness, and the resulting acceleration and displacements at the identified nodes were recorded. While the model includes springs in both x and y directions, earthquake motions were only applied in x direction. A large distance between fixation points of spring connectors at the caisson and at the boundary was modelled to avoid interactions from the axial motions inducing forces into the lateral springs or lateral motions introducing forces in axial springs.

3.3. Soil model

The soil structure interaction model used for the calibration towards the centrifuge test results was based on the work already started for the Shah Deniz project. The goal was to develop a soil model to be used for time series earthquake analyses that accounted for soil non-linearity and provided a realistic hysteretic damping for cyclic loading. Distributed non-linear springs along the four caissons for each of the three directions of translation were introduced. The springs include a backbone curve characterising the initial loading and simulate unloading-reloading in a manner that provides realistic damping [22]. A hysteretic model where unloading-reloading follows the Masing rule is realistic for a loading situation with oscillations around zero load, or with a low static average load, where increasing average displacements (ratcheting) is not expected. The Masing rule applied to a non-linear spring defines that if a load reversal occurs at a point defined by (y,p), the load-deformation curve is identical to the shape of the backbone curve but enlarged by a factor of 2.

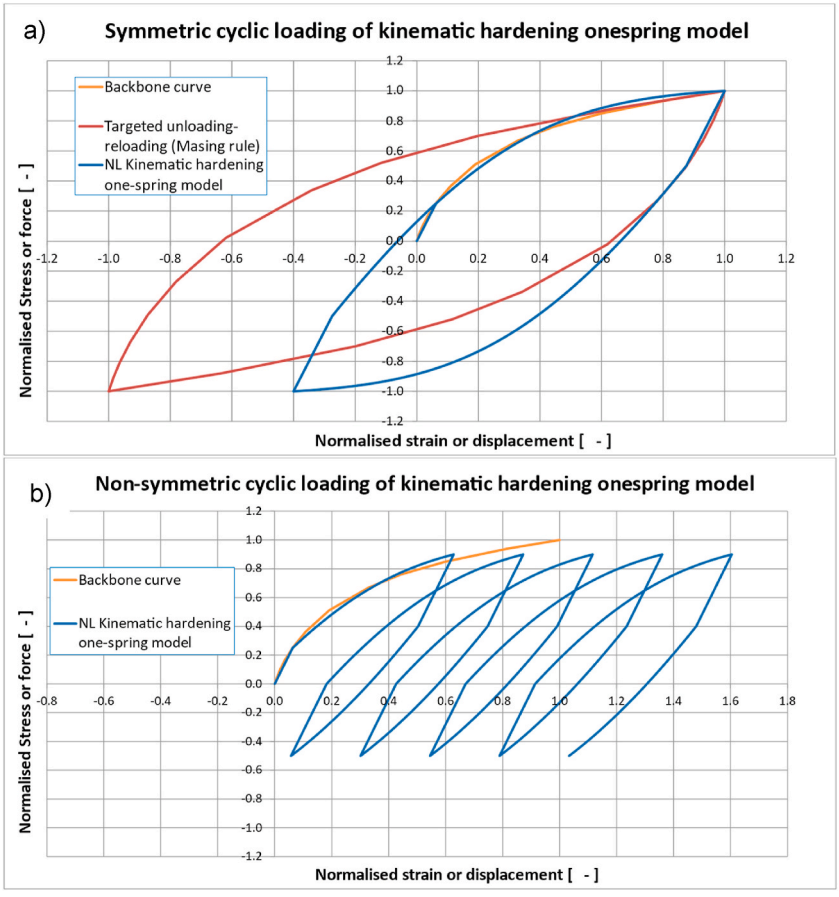

Fig. 9. Performance of kinematic hardening model for symmetrical cyclic loading (a) and cyclic loading about a non-zero average (b).

Within the program ABAQUS used for the time series analyses the kinematic hardening model is available which for materials describe both the elastic stiffness as well as the non-linear relation between stress and plastic strain beyond the defined yield stress. A similar kinematic hardening model is available to connectors (springs) giving the non-linear relation between force and relative plastic motion beyond the defined yield force.

The plasticity formulation in ABAQUS connector elements is equal to the plasticity formulation in metal plasticity. The kinematic hardening component is defined to be a combined effect of a purely kinematic term (the linear Ziegler hardening law) and a relaxation term that introduces the nonlinearity. Thus, the kinematic hardening model is defined via the yield value and the hardening parameters, initial kinematic hardening modulus, C and the parameter γ, that determines the rate at which the kinematic hardening modulus decreases with increasing plastic deformation, ref. [23]. It should be noted that metallic models behave differently in comparison with soil behaviour, especially when subjected to cyclic loading and in particular regarding accumulation of plastic strains.

A single connector with kinematic hardening material model may be chosen to fit the backbone curve for initial loading, however for the cyclic loading, such a single connector will overestimate permanent displacements. For a pure symmetrical cyclic loading, a single kinematic hardening connector will result in a permanent displacement for the first cycle, which however does not increase for following cycles. This is shown on Fig. 9a, where symmetric loading performance of a single kinematic hardening connector is compared with a Masing rule type model, more realistic for soil. For loading situations where there are static permanent loads together with cyclic loading, the kinematic hardening model with a single connector will also overestimate the accumulated permanent displacements resulting from the cyclic loading. This general performance is shown on Fig. 9b. The problem with too large permanent displacements for a single connector can be resolved by introducing multiple connectors in series, all with a kinematic hardening model. Bilinear models for each connector with different yield points, where the parameter C representing linear hardening beyond yield, can be used to match a prescribed backbone curve and a corresponding unloading-reloading hysteresis. This modelling, where the γ parameter is set to zero for each of the springs, gives no gradual increase of permanent displacements during cycling. One of the connectors should have a yield point equal to the maximum resistance intended for the resulting soil spring and with close to zero inclination of the linear hardening. The principle of such series connected springs for simulation of the backbone curve is shown in Fig. 10. Here the yield points for the four springs have been chosen at normalised stress/force of 0.25, 0.5, 0.75 and 1.0. Using four springs in series captures the target stress-strain or force-displacement relationship sufficiently well for the purpose of the earthquake analyses. Adding more springs would essentially converge towards the desired Masing rule.

The performance of the individual springs and the resulting performance of the series coupled springs can be demonstrated in a simple spread sheet program for calibrating the model parameters for input to the earthquake analysis program. The input parameters for a kinematic hardening material are the elastic modulus, D, the yield point, σ_y, the linear hardening, C, and the parameter for non-linear hardening, γ. An incremental development of the material performance for uniaxial loading involves the following calculations for each step, i, where σ_i is the actual stress and α_i is the stress in excess of the yield stress:

$$\sigma_i = \sigma_{i-1} + d\sigma_i \tag{1}$$

$$\varepsilon_{el,i} = \sigma_i / D \tag{2}$$

$$d\alpha_i = sign(d\sigma_i) \bullet \left(|\sigma_i - \alpha_{i-1}| - \sigma_{yield}\right) \quad when\ |\sigma_i - \alpha_{i-1}| > \sigma_{yield} \tag{3}$$

$$= 0 \quad when\ |\sigma_i - \alpha_{i-1}| \le \sigma_{yield}$$

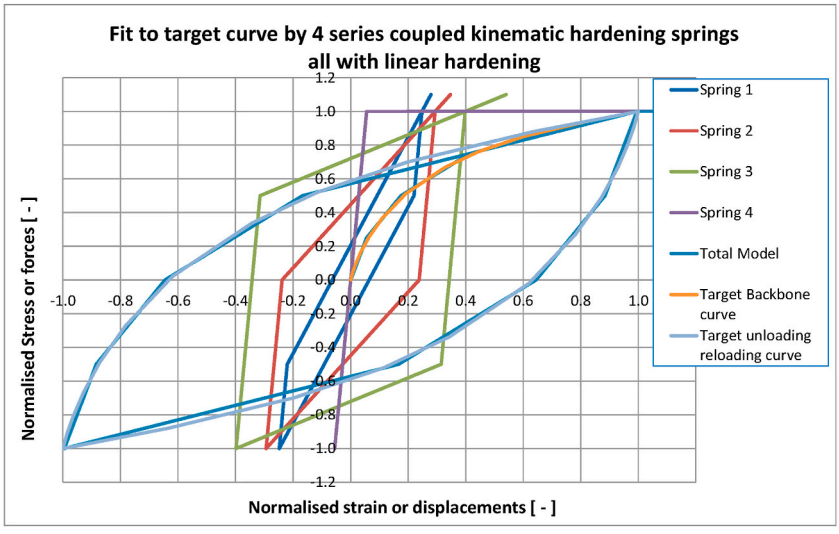

Fig. 10. Unloading-reloading sequence with 4 series coupled springs compared to the Masing rule.

$$\alpha_i = \alpha_{i-1} + d\alpha_i \tag{4}$$

$$d\varepsilon_{pl,i} = \frac{d\alpha_i}{C - \gamma \bullet \alpha_i} \quad when \quad \sigma_i > \alpha_i \tag{5}$$

$$= \frac{d\alpha_i}{C + \gamma \bullet \alpha_i} \quad when \quad \sigma_i < \alpha_i$$

$$\varepsilon_{pl,i} = \varepsilon_{pl,i-1} + d\varepsilon_{pl,i} \tag{6}$$

$$\varepsilon_i = \varepsilon_{el,i} + \varepsilon_{pl,i} \tag{7}$$

when each of the spring connectors are assigned the same length, the normalised force (P/P_{max}) versus normalised displacement (Y/Y_{max}) for the resulting series coupled spring connector becomes the same as the normalised stress versus sum of normalised strain for the material assigned to the spring connectors. The calibration for a series coupled spring is thus performed using above formulation adding the normalised strain, ε_i, for each spring connector material corresponding to the normalised stress, σ_i.

Assigning a value higher than zero to the γ parameter results in an accumulation of displacements for the spring when the cycling exceeds the yield point. When a series of springs are included with non-linear hardening assigned to one of them only, the model can be better controlled with respect to the accumulation of plastic strains (displacements). The model must be tuned to achieve a realistic accumulation of strains/displacements for an expected typical equivalent load, i.e. number of cycles at a relevant level of average stress/load and cyclic stress/load amplitude. Assuming full correlation between relative strains and displacements (relative to their values at failure) and between relative stresses and loads, one may use cyclic strain contour diagrams relevant for the soil in question for the calibration of the connector that includes non-linear hardening. An example of such diagram is shown in Fig. 11. Further guidance and examples on cyclic soil performance is provided by K [24]. Fig. 12 (a,b) shows examples of symmetric cyclic loading and non-symmetric cyclic loading applied to four series coupled springs where one spring includes non-linear hardening and the three others pure linear hardening.

For the centrifuge test the following normalised parameters (Table 2) were defined for the four spring connectors.

As an alternative to using series coupled springs to match the intended performance of the resulting spring, parallel coupled springs may equally well be used. Whereas when combining springs in series the sum of displacement should be controlled for given loads, the sum of forces should be checked for given displacements if using parallel coupled springs.

As the centrifuge testing was performed as part of the design process, work had already been performed to establish soil springs for the Shah Deniz structures. The non-linear lateral stiffness was calculated from various approaches, starting off by defining the lateral backbone curve from traditional ISO p-y curves. It is generally recognized that the ISO p-y model (ISO 19901–2) for clay may underestimate the resistance and overestimate the displacements required to mobilize the resistance for large diameter piles. P-y curves with large diameter corrections, as suggested by Stevens J.B and Audibert J.M.E [25] was also calculated. As pointed out by Ref. [14] it is not logical that resistance normalised with the z/D ratio should be dependent on the actual diameter. The approach suggested by

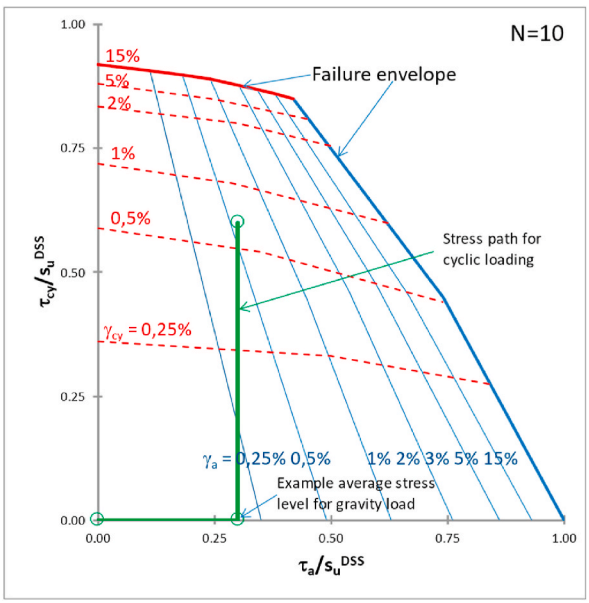

Fig. 11. Example of stress/strain contour diagram for combined average and cyclic loading.

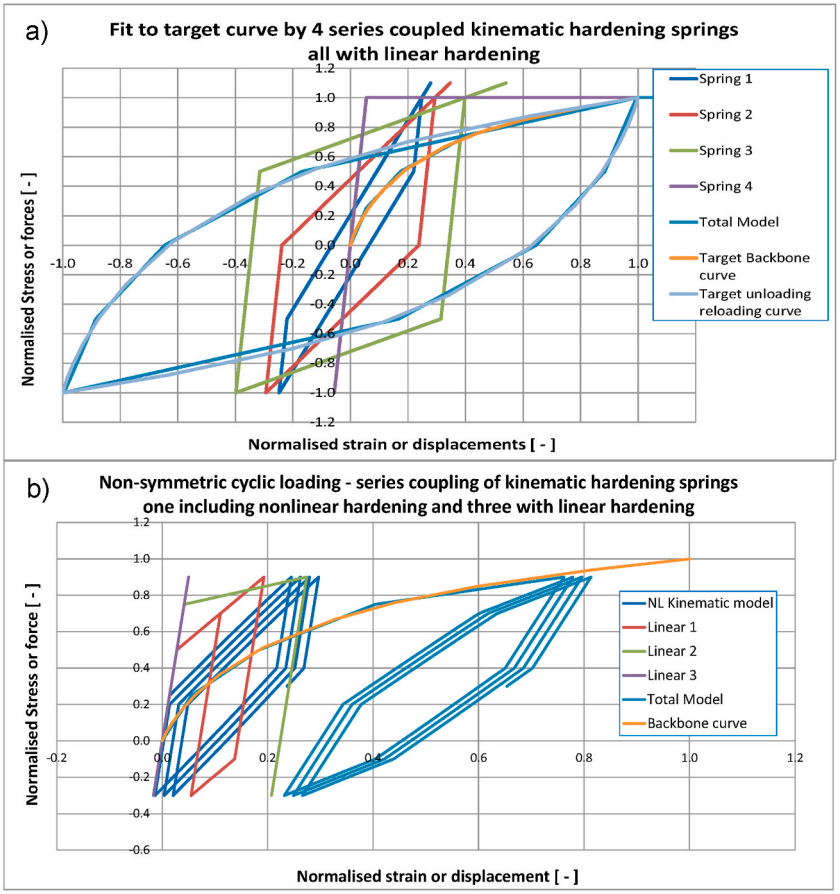

Fig. 12. An example of symmetric cyclic loading (a) and non-symmetric cyclic loading (b) applied to four series coupled springs, where one of the springs includes nonlinear hardening.

Table 2
Normalised kinematic hardening parameters applied for the centrifuge test analyses.

$$D_{connector} = \frac{D_{ref} \bullet P_{max}}{Y_{max} \bullet L_{connector}}$$

$$P_{yield,connector} = \sigma_{y,ref} \bullet P_{max}$$

$$C_{connector} = \frac{C_{ref} \bullet P_{max}}{Y_{max} \bullet L_{connector}}$$

$$\gamma_{connector} = \frac{L_{connector}}{Y_{max}} \bullet \gamma_{ref}$$

Normalised parameters	Spring1	Spring2	Spring3	Spring4
Normalised yield stress, $\sigma_{y,ref}$	0.25	0.50	0.75	1.00
Normalised Youngs modulus, D_{ref}	18	18	18	18
Normalised linear hardening, C_{ref}	3.50	2.50	0.72	0.05
Normalised non-linear hardening, γ_{ref}	0.61	0.00	0.00	0.00

The normalised parameters provide the curve describing the relation between Y/Y_{max} and P/P_{max}. When giving input for springs in the actual analyses, the normalised values are modified as follows, where P_{max} is the maximum force for the spring and Y_{max} is the displacement at which maximum force is reached.

Jeanjean was also used for the comparison. Realising the uncertainty of above approaches applied to the dimensions of the Shah Deniz caisson with large diameter and low ratio of diameter to penetration depth, 3D finite element analyses were initiated. These were performed with PLAXIS 3D program with the soil model calibrated to laboratory tests on the site-specific clay consisting of consolidated triaxial compression and extension as well as consolidated DSS tests performed. The anisotropic NGI-ADP model in PLAXIS 3D

was applied with nonlinear stress-strain characteristics fitting the laboratory tests. Analyses were performed for a single caisson as well as for two adjacent caissons, to investigate the group effect of the closely spaced foundations.

A comparison of the finite element results with the curves based on the ISO and Jeanjean p-y curves are shown in Fig. 13. The PLAXIS 3D analyses were run by applying a pure horizontal displacement of the foundation caisson(s). The resistance corresponding to the p-y curve concepts shown on Fig. 13 are the integrated p-y resistances from top to bottom of the caisson. The p-y curves are calculated based on the static curves for the methods but scaled with the cyclic strength correlations interpreted from cyclic DSS tests (Fig. 3). Low and high factors of 1.0 respectively 1.4 were applied for the Shah Deniz soil.

The PLAXIS 3D analysis for a single caisson resulted in higher resistance than the p-y curve calculations (Fig. 13, dotted purple curve). This may be explained by the horizontal shear resistance underneath the caisson, which were not included in the p-y calculations but is explicitly accounted for in the PLAXIS analyses. When accounting for group effects in the PLAXIS 3D analyses the resistance per caisson reduced to become comparable with that from the p-y curve calculations (Fig. 13, green curve). It is seen that using the uncorrected ISO formulations gives a too soft behaviour (Fig. 13, dotted brown curve). The Jeanjean method correlates the stiffness of the curves to the small strain $G_{max,}$ and proves to be very sensitive to that parameter, actually more than proportional to the G_{max} value.

As a result of the fit with the PLAXIS 3D analyses it was decided to use the modified ISO p-y curves as basis for modelling of the lateral soil connectors. It is recognized that basing the non-linear resistance on the ISO formulations modified for large diameter effects does not explicitly reflect the physics involved, as there is no obvious reason why a normalised resistance should be diameter dependent, effect of cyclic loading is not realistically accounted for and group effects between adjacent caissons are not considered. However, the outcome of the curves, when applying the correction for the large diameter effect, making corrections for cyclic loading, and varying the input ε_{50} parameter, turns out to agree reasonably well with the PLAXIS 3D analyses accounting for group effects. It was observed that the calculated damping when using the modified ISO p-y curve as the backbone curve became somewhat higher than the values from cyclic laboratory tests. Therefore, the shape of the P–Y curve was slightly adjusted in order to achieve realistic hysteretic damping. The adjusted backbone curve resulted in a damping of 28% for oscillations reaching maximum resistance with gradually reduced damping for lower oscillation amplitudes.

For the validation analyses based on the centrifuge test conditions a best estimate correction factor of 0.7 was used for the cyclic shear strength, as illustrated on Fig. 3. It should be noted that the choice of using the modified ISO approach for the p-y curves is specifically made for the foundation solution of the Shah Deniz manifold, chosen because it matched the 3D PLAXIS analyses, and is not meant to be generally applicable to any foundation design and design condition. In general, it is recommended that 3D finite element analyses are used for calibration of simplified spring models.

With the spring connector being made up by four connectors the resulting yield point was set at 25% utilisation of the maximum resistance. Below that the connector behaved elastic. In order to account for some damping for cyclic amplitudes lower than 25% of maximum, linear dashpot dampers were added acting together with the springs, connected in parallel to the spring. The damping coefficient was set to provide 3% damping at an oscillation period of 1sec.

The vertical resistance was modelled with spring connectors in the same manner as for the horizontal resistance with 4 connectors

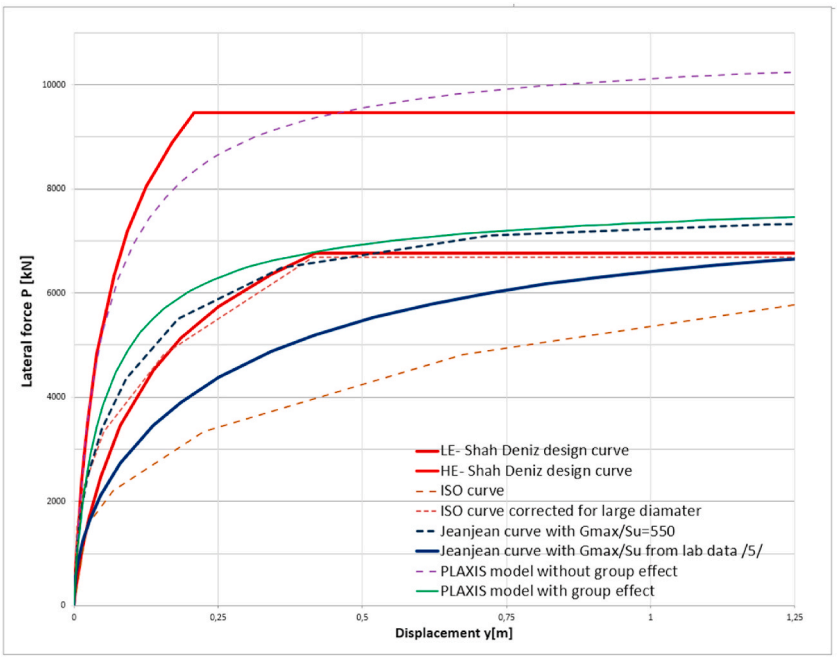

Fig. 13. Comparison of lateral resistance calculated from various approaches for Shah Deniz.

in series and a dashpot damper in parallel for each support node. The same relative shape of the backbone curve was used, assuming outer skin friction to be mobilised at 1% of the diameter and end bearing at 10% of the caisson diameter.

For this 4-caisson foundation system, the main contribution for resisting overturning is provided by the differential vertical resistance between the caissons. This is more important than the contribution from differential vertical reaction across the base of the individual caissons. Therefore, no additional springs for capturing moment resistance on indvidual caissons were judged necessary. Also, the mobilisation of vertical resistance on the individual caissons are low for the earthquake loading. This is mainly because of a design requirement that all permanent vertical loads should be resisted by skin friction along the caisson walls only. For the rapid earthquake loading, fully plugged end bearing can be mobilised. The outcome is a modest mobilisation of the vertical end bearing capacity. This is also a reason for why no further work for calibration of vertical spring models were performed.

4. Results and discussions

4.1. Calibration of soil stiffness for horizontal response

Recorded earthquake time histories were applied at the outer boundary of each of the assembled (series coupled) spring connectors in ABAQUS. The backbone curve for the lateral soil springs were calculated from the modified ISO approach, initially assuming $\varepsilon_{50} = 1.5\%$ as were used for the Shah Deniz soil. Comparing calculated versus recorded response presented by UC Davis [26]; $\varepsilon_{50} = 1.0\%$ was found to give a better fit. This is reasonable as the less plastic mixture of Shah Deniz clay with kaolin should mobilize the resistance at lower displacements compared to the pure Shah Deniz clay.

4.2. Comparison between ABAQUS results and recorded motions - ALE earthquake

Accelerometers # A14 to # A20 are the ones attached to the manifold, see Fig. 6. Displacements are calculated by double integration of the recorded accelerations. The acceleration and displacement plots (Fig. 14 through Fig. 18) show that the recorded and calculated response is generally in a good agreement. There is a particular good fit between analysed and recorded horizontal motions, seen from Fig. 14, Fig. 15 andFig. 16.

The accelerometers A15 and A16 are mounted symmetrically about the axis for the direction of the imposed earthquake motions. As such, and because the structural model is symmetric about the same axis, the analysed motions at those points are, as they should be, exactly the same. The recorded motions are also remarkably equal. Also, the motions from A17 situated at opposite side of the manifold from A15 and A16 are practically the same, the slight difference being due to minor rotation of the structure. While the maximum response is remarkably well captured by the analysis, eigen-period motions are triggered in the analyses which is not seen equally well in the recorded motions. This informs that the assigned 3% damping for cyclic amplitudes below the modelled yield point is too low. This is however not seen to have had any impact on the maximum response.

One difference is that the analysed displacements end with displacements different from zero, whereas the recorded displacements as presented all end with zero displacements. This is because all recorded acceleration time histories had been ‘baseline corrected’ to get zero displacement at the end. This is a necessity since only a minor change in acceleration early in the time history can when integrating result in large unrealistic displacements. Integration of recorded accelerations provide reliable cyclic displacements, but cannot be used to determine final displacements, The horizontal linear potentiometers intended for measuring displacements could unfortunately not be relied upon due to improper contact onto the structure. As a back-up UC Davis performed image analyses for 5 corners. These had an accuracy of 0.05 m with analysed values between 0 and 0.10 m for the 5 corners. Thus, it is difficult to compare the values of permanent displacements for any calibration purpose. However, all points had permanent displacements from the image analyses in the same direction as predicted by the FE-analysis, indicating that there was a real although small permanent horizontal displacement resulting from the earthquake.

For the vertical motions recorded by the accelerometers # A18 to # A19 (See Fig. 17 through Fig. 18), the fit between the recorded data and calculated response did not appear equally good as for the horizontal direction.

One difference is that in the ABAQUS analyses displacements due to the static weight are included whereas the presented monitored displacements are zero at the start of the earthquake. Those displacements are therefore subtracted when presenting the results from the analyses. Comparing measured and analysed vertical displacements it is seen that after the first major downward displacement, a permanent displacement results, which is not seen from the monitored displacements. This can be explained by the difference in how skin friction is mobilised prior to the earthquake. Since the structure for the centrifuge test is installed by pushing it into the soil, the skin friction has been fully utilised and thereafter unloaded. Thus, skin friction can be remobilised at relatively small displacements. The installation has not been simulated in the analyses and skin friction is only mobilised from the weight of the structure. When pushed further downwards the friction response moves along the backbone curve and results in permanent displacements when unloaded. Apart from the difference in permanent displacements the cyclic amplitudes for the larger motions are very comparable.

The recorded vertical displacements also all end with zero displacements as for the horizontal displacements, due to baseline corrections. It is seen that the vertical motions are an order of magnitude lower than the horizontal. The eigen-period of the entire system was evaluated based on the cyclic motions from both FEM and centrifuge models. The comparison between these two eigen-periods shows a good agreement, which is around 0.7–0.8 s for both cases.

It can be concluded that the soil spring model used in our ABAQUS analyses are able to simulate the global response of the soil-structure system under the earthquake load accurately.

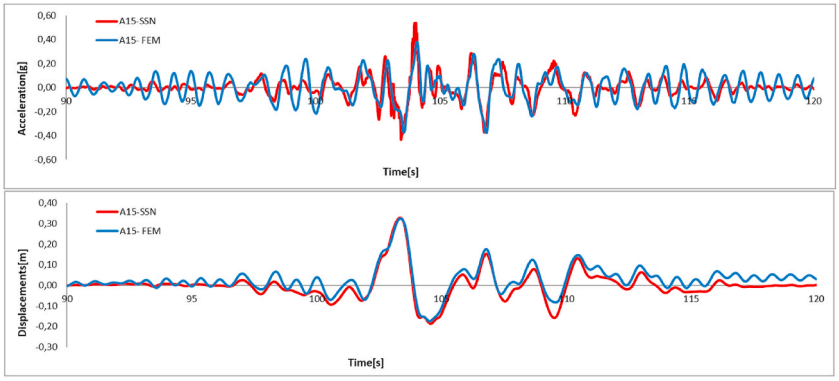

Fig. 14. ALE#1- Comparison between FEM and instrument #A15 - (Horizontal direction).

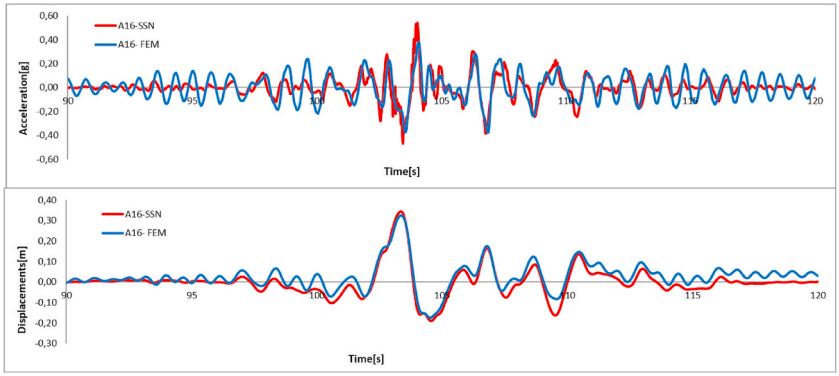

Fig. 15. ALE#1- Comparison between FEM and instrument #A16 - (Horizontal direction).

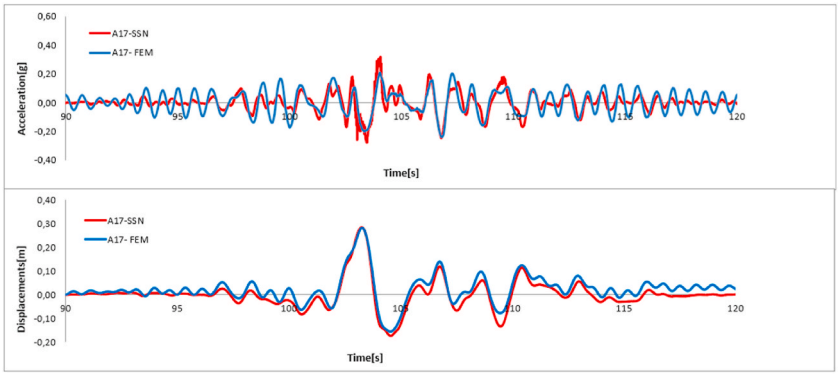

Fig. 16. ALE#1- Comparison between FEM and instrument #A17 - (Horizontal direction).

4.3. Extension of model used in design analyses and relevant findings

The approach for determining non-linear soil springs as described in this paper was after the successful validation exercise applied for the detail design of the manifold structures at Shah Deniz. Extensions to the model that were implemented for final design and the results are summarised below.

- A complete model of the manifold structure was established for the final analyses, including details such as the support frame, surrounding protection frame, the piping system, valves, supports and the hubs for connection of external flowlines/well jumpers. These elements were modelled with their actual properties to capture their dynamic performance.

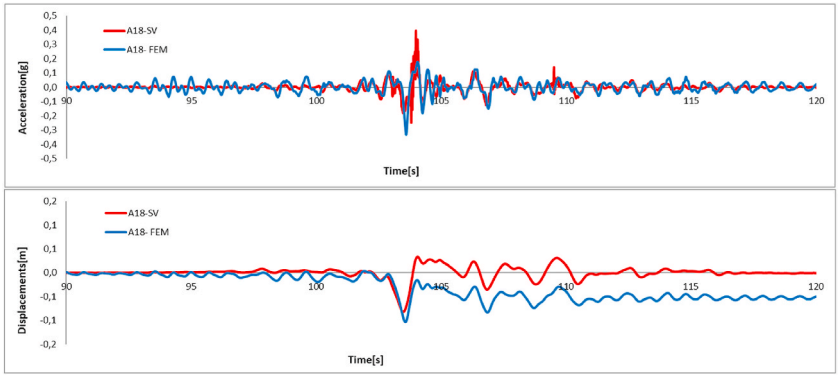

Fig. 17. ALE#1- Comparison between FEM and instrument #A18 - (Vertical direction).

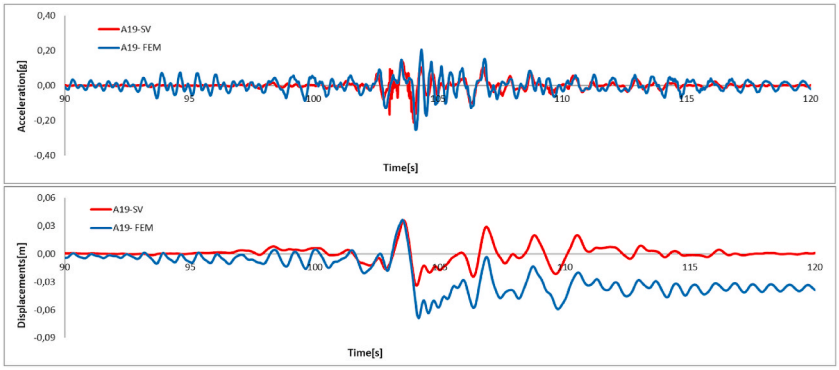

Fig. 18. ALE#1- Comparison between FEM and instrument #A19, corrected for the initial static settlement (vertical direction).

- The earthquake motions used in the centrifuge test were based on the Northridge earthquake. For the Shah Deniz design analysis seven different time histories scaled for the Shah Deniz field were analysed in accordance with the requirements of the ISO 19901–2 code.
- High and low estimates of soil conditions and added mass from water was evaluated and modelled to understand the sensitivities to the various parameters and capture the full range of potential responses within the structure.
- Earthquake was the final load step in a sequence of load steps for installation and normal operation, such as placement on seabed, pull-in and connection at the hubs and application of production temperature and pressures, all steps modelled explicitly in ABAQUS to obtain realistic initial conditions prior to an earthquake event.
- The analyses resulted in overutilization of a few pipes and supports on the manifold, implying a risk of leakage during an earthquake event. These pipes and supports were then redesigned and found acceptable in a new set of analyses. Thus these analyses proved important for design of the manifold and its system of piping and valves.
- Other than the hubs, the external pipes (flexible jumpers from the surrounding production wells and export flowline) were not included in the manifold analyses in order to limit the complexity of the analyses. Since the dynamic mass of these pipes were very low compared to those of the manifold, the external pipes would not influence the motions of the manifold. Instead, independent analyses were performed for each of the external pipes, where the motions at the manifold hubs resulting from the manifold analysis were used as boundary. Earthquake was here the final load step in a sequence of load steps for installation and normal operation, such as placement on seabed, pull-in and connection at the hubs and application of production temperature and pressures, all steps modelled explicitly in ABAQUS to obtain realistic initial conditions prior to an earthquake event.
- Kinematic hardening type springs were used to represent the pipe-soil interaction (vertical, axial and lateral) for connected flowlines and well jumpers. The springs were bilinear or trilinear including also unloading and reloading. Earthquake motions were applied to the far boundary of the lateral springs.
- These analyses proved important for design of the hub connections and of the transition elements between the hubs and the pipes.

5. Summary and conclusions

Centrifuge tests and subsequent back-analyses were conducted to develop a procedure for establishing non-linear soil springs with hysteretic damping to represent the soil-structure interaction of a 4-caisson supported manifold subsea structure under earthquake

loading.

The major findings are summarised below.

- In soft clay, in addition to the varying amplitudes with depth, there is a phase difference of the horizontal motions up through the soil owing to the low shear wave velocity. This phase difference was demonstrated through the monitoring of soil motions in the test bin and is relevant to consider for earthquake analyses of structures supported on foundations deeply embedded in soft clays. These depth varying motions were accounted for in the validation analyses.
- Non-linear hysteretic soil resistance models were constructed by use of several (here four) spring connectors assigned kinematic hardening material properties and connected in series to form the resulting non-linear hysteretic spring connector. A dashpoint damper was modelled in parallel with the spring connector to provide some damping within the initial linear part of the spring.
- The soil model used for the calibration analyses was based on a preceding study made for the manifold foundations and soil conditions at the Shah Deniz field, comparing different approaches for calculation of lateral p-y curves with geotechnical 3D finite element analyses with non-linear soil modelling based on laboratory tests.
- The manifold structure for the centrifuge test was designed to obtain a realistic mass distribution, i.e. total mass with CoG and mass moment of inertia. The structure was rigid. Implementation of the manifold structural elements or of piping and other equipment is not feasible for the centrifuge test. The flexibility and corresponding dynamics of those have, however, no significant impact on global motions for this type of structure, which was the main focus for the test.
- The fit between the recorded and calculated response of the centrifuge test was generally very good, in particular when comparing horizontal displacements.
- In the analyses eigen-period oscillations were triggered, which were not observed equally clear from the records. This informs that the damping assigned to the dashpot damper was too low. The maximum response did however not seem to be influenced by that.
- From the comparisons made between recorded and analysed response from the centrifuge tests it was concluded that the soil resistance model intended for the Shah Deniz site specific earthquake analyses captured the important features of the soil behaviour and hence could be applied in detailed design analyses.

Declaration of competing interest

The authors declare that they have no known competing financial interests or personal relationships that could have appeared to influence the work reported in this paper.

Data availability

Data will be made available on request.

Acknowledgements

The authors would like to acknowledge Centre for Geotechnical Modelling in Davis university for model test, Erik Sørlie and Pauline Suzuki, former DNV, Norway, for his support in developing soil springs concept, Ramin Moselmian, Jørn Hennig, Liv Hamre and Jan Holme from DNV, Norway, also Airaf Patel and Daniel Simkin from BP for their support during the project.

References

[1] Byrne BW. Investigations of suction caissons in dense sand. PhD thesis. Oxford, UK: University of Oxford; 2000.
[2] Johansson P, Aas P, Hansen S. Field model tests for a novel suction anchor application, in '6. In: International symposium on field measurements in geomechanics; 2003. p. 145–53. Oslo, Norway.
[3] Kelly RB, Houlsby GT, Byrne BW. A comparison of field and laboratory tests of caisson foundations in sand and clay. Geotechnique 2006;56(9):617–26.
[4] Zhu B, Byrne BW, Houlsby GT. Long-term lateral cyclic response of suction caisson foundations in sand. J Geotech Geoenviron Eng 2013;139(1):73–83. https://doi.org/10.1061/(asce)gt.1943-5606.0000738. Available at:.
[5] Cox JA, O'Loughlin C, Cassidy M, Bhattacharya S, Gaudin C, Bienen B. Centrifuge study on the cyclic performance of caissons in sand. Int. journal of Physical modelling in geotechnics 2014;14(4):99–115.
[6] Foglia A, Ibsen LB, Nicolai G, Andersen LV. Observations on bucket foundations under cyclic loading in dense saturated sand. In: Gaudin C, White D, editors. ICPMG2014 – physical modelling in geotechnics: proceedings of the 8th international conference on physical modelling in geotechnics, perth, Australia. Boca Raton, FL, USA: CRC Press; 2014. p. 667–73.
[7] Jostad H, Andersen K, Khoa H, Colliat J. Interpretation of centrifuge tests of suction anchors in reconstituted soft clay. In: Meyer V, editor. Frontiers in offshore geotechnics III; 2015. p. 269–76. Oslo, Norway.
[8] Athanasiu C, Bye A, Tistel J, Ribe A, Arnesen K, Feizikhankandi S, Sørlie E. Simplified earthquake analysis for wind turbines and subsea structures on closed caisson foundations, Frontiers in offshore geotechnics III. 2015. 221.
[9] Tran MN. Installation of suction caissons in dense sand and the influence of silt and cemented layers, PhD thesis. Sydney, Australia: The University of Sydney; 2005.
[10] Houlsby GT, Byrne BW. Design procedures for installation of suction caissons in clay and other materials. Proc Inst Civ Eng: Geotech Eng 2005;158(2):75–82.
[11] Andersen KH, Jeanjean P, Luger D, Jostad HP. Centrifuge tests on installation of suction anchors in soft clay. Ocean Eng 2005;32(7):845–63. https://doi.org/10.1016/j.oceaneng.2004.10.005.
[12] Stapelfldt M, Bienen B, Grabe J. Centrifuge tests investigating the effect of suction caisson installation in dense sand on the state of the soil plug. Proceedings of the 9th. [S.l.]. In: Physical modelling in geotechnics. vol. 1. UK: CRC Press; 2018. S. 669–674.
[13] Chen W, Randolph MF. Centrifuge tests on axial capacity of suction caissons in clay. Proceedings, International Symposium on Frontiers in Offshore Geotechnics 2005:243–9.

[14] Jeanjean P, Znidarcic D, Phillips R, Ko HY, Pfister S, Cinicioglu O, Schroeder K. Centrifuge testing on suction anchors: double-wall, over-consolidated clay, and layered soil profile, proceeding, annual offshore technology conference. 2006. Paper OTC 18007.
[15] Gelagoti F, Georgiou I, Kourkoulis R, Gazetas G. Nonlinear lateral stiffness and bearing capacity of suction caissons for offshore wind-turbines" Ocean Engineering, vol. 170; 2019. p. 445–65. https://doi.org/10.1016/j.oceaneng.
[16] Zheng BL, Kutter BL, Hirt GS, Zhou YG, Wilson DW, Clukey EC. Centrifuge modelling of seismic behaviour of caisson-supported subsea manifold on soft clay, proceeding of 6th international conference on earthquake geotechnical engineering. 2015 [Christchurch, New Zealand].
[17] Feizi S, Arnesen K, Moselmian R. Calibration analysis report for FMC Kongsberg Subsea AS, DNVGL report # 2015-0847. 2016.
[18] Feizi S, Arnesen K, Andreas A, Moselmian R. Earthquake analysis report for FMC Kongsberg Subsea AS, DNVGL report # 2015-0748. 2017.
[19] ISO 19901-2. Petroleum and Natural Gaz Industries-specific requirements for offshore structures, Part2, Seismic design procedures and criteria. 2004.
[20] ABAQUS-CAE. Standard Version 6.11. 2012.
[21] PLAXIS program. 2016.
[22] Vucetic M, Dobry R. Effect of soil plasticity on cyclic response. Journal of Geotechnical Engineering 1991;117(1).
[23] Besseling JF. A theory of elastic, plastic, and creep deformations of an initially isotropic material showing anisotropic strain-hardening, creep recovery, and secondary creep. J Appl Mech 1958:529–36.
[24] Andersen KH. Cyclic soil parameters for offshore foundation design, Frontiers in Offshore Geotechnics. ISFOG; 2015.
[25] Stevens JB, Audibert JME. Re-Examination of p-y curves formulation. USA: OTC 3402; 1997.
[26] Zheng BL, Hirt GS, Kutter BL, Wilson DW, Zhou YG. Soil structure interaction of caisson-supported subsea manifold and wellhead on soft clay: centrifuge data report for BLZ02/PHASE 3-#2." technical report, 1.02. Davis: University of California; 2014.